

Grain-boundary buckling and spin-glass models of disorder in membranes

Carlo Carraro and David R. Nelson

Department of Physics, Harvard University, Cambridge, Massachusetts 02138

(Received 2 July 1993)

A systematic investigation is presented of grain boundaries and grain-boundary networks in two-dimensional flexible membranes with crystalline order. An isolated grain boundary undergoes a buckling transition at a critical value of the elastic constants, but, contrary to previous findings, the shape of the buckled membrane is shown to be asymptotically flat. This is in general not true in the case of a network of intersecting grain boundaries, where each intersection behaves as the source of a long-range stress field. Unlike the case of isolated dislocations or disclinations, the energy associated with these stresses is finite; they can, however, destabilize the flat phase. The buckled phase can be modeled by an Ising spin glass with long-range antiferromagnetic interactions. These findings may be relevant to the understanding of the wrinkling transition in partially polymerized vesicles reported in recent experiments.

PACS number(s): 87.22.Bt, 46.30.Lx

I. INTRODUCTION

Flexible membranes are two-dimensional (2D) generalizations of linear polymer chains. The properties of a 2D membrane, embedded in three-dimensional space, depend strongly on the internal order, crystalline, hexatic, or fluid. As in other realizations of 2D matter, defects, and their interactions, affect crucially the stability of a given phase. For example, the melting transition in two dimensions can be described as proliferation of topological defects [1]. A membrane, however, is not confined to a plane. Thus, although the stable phase of a defect-free crystalline membrane at low temperature is flat, strains induced by a defect, such as a dislocation, can be accommodated by displacements in the normal direction, resulting in the buckling of the membrane [2]. This process entails a trade-off of in-plane stretching energy for curvature energy, and, hence, it occurs when

$$\frac{K_0 l^2}{\kappa} \geq \gamma. \quad (1)$$

Here, K_0 is Young's modulus, κ is the bending rigidity, l is a length scale, and γ is a dimensionless constant of order 10^2 . In membranes of size R , $l=R$ for disclinations, and $l=\sqrt{Rb}$ for a dislocation with Burger's vector \mathbf{b} . Thus, these defects always buckle in sufficiently large membranes, irrespective of the value of the elastic constants.

This conclusion, however, does not hold for finite energy defects such as vacancies, interstitials, or tightly bound dislocation pairs. In this case, l is of order a lattice constant, and thus the stability of the flat phase in the presence of such defects is determined by the actual value of the elastic constants. This brings about the interesting possibility of a buckling transition in an infinite system as a function of temperature. Because κ typically increases with temperature, while K_0 decreases, the condition (1) may be associated with a boundary in the (l^2, T) plane, separating buckled and flat regimes (see Fig. 1).

Recent studies of membranes with defects and quenched random disorder have been prompted in part by experiments of Mutz, Bensimon, and Brienne [3], showing that partially polymerized vesicles undergo a (possibly first-order) reversible phase transition from a high-temperature phase characterized by a smooth, "floppy" surface, to a low-temperature phase where the vesicles appear rigid and highly wrinkled. This wrinkling transition has been likened to the spin-glass transition of magnetic systems [3,4]. To understand the mechanism of the transition, it is helpful to observe that the effect of the partial polymerization is to nucleate microcrystalline domains around polymerized patches. Upon cooling, crystalline order arises in the unpolymerized material surrounding these domains. This has led to speculation that the grain boundaries, resulting when microcrystals

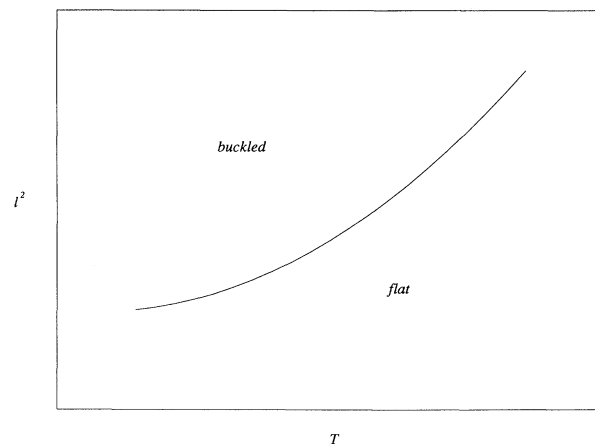


FIG. 1. The temperature behavior of the elastic constants of a membrane can cause finite energy defects, such as vacancies, interstitials, or grain boundaries, to buckle as the temperature is lowered. Buckling will occur at higher temperatures for defects characterized by a larger length scale, according to Eq. (1). Thus, low angle grain boundaries will buckle first upon cooling a polymerized grain-boundary network.

with different orientations meet, may be responsible for the observed wrinkled structure. The following argument was given to support this scenario [5].

Consider a low-angle grain boundary in a 2D crystal. This can be viewed as a row of dislocations, with Burger's vector \mathbf{b} perpendicular to the boundary. Let θ be the boundary tilt angle. The spacing between dislocations, h , is then given by Frank's law [6], $h = b / 2 \sin(\theta/2) \approx b / \theta$. On length scales large compared to h , the stress fields of the dislocations are screened exponentially, provided the average Burger's vector is strictly perpendicular; on shorter length scales, however, the behavior of the grain boundary should be dominated by the individual dislocations. Computer simulations of tethered membranes [2] have shown that isolated dislocations in a finite membrane of size R destabilize the flat phase, provided that $R > 127\kappa / K_0 b \equiv R_B$, consistent with Eq. (1) with $l = \sqrt{Rb}$. Hence, one might expect that, if $h > R_B$, the grain boundary will buckle out of flat space, possibly taking the shape of a rippled hinge, possibly with large out-of-plane displacements, which would then appear as wrinkles.

The present work is devoted to a systematic study of grain boundaries and grain-boundary networks in two-dimensional flexible membranes with crystalline order. While we find that an infinite grain boundary does indeed undergo an intriguing second-order transition from a flat to a corrugated phase as the ratio of the bending rigidity to the shear modulus or tilt angle is varied, we show that the out-of-plane displacement decays exponentially away from the boundary, i.e., the shape of the membrane remains asymptotically flat. We also find, however, that this conclusion does not hold in the case of a network of intersecting grain boundaries, where each intersection behaves as the source of a long-range stress field, e.g., as a disclination multipole. Unlike the case of isolated dislocations or disclinations, the energy associated with these stresses is generally finite; they can, however, cause buckling at a sufficiently low temperature, determined by the size l of the (localized) multiple source.

Thus, upon cooling of a polycrystalline membrane, in which a grain-boundary network has formed, one expects a hierarchy of buckling transitions to take place, with the low-angle grain boundaries puckering first, followed by the high-angle ones (low-angle grain boundaries correspond to very large values of l^2 in Fig. 1). Eventually, as the network of buckled grain boundaries begins to percolate across the membrane, the (pointlike) grain-boundary nodes will buckle, causing large wrinkles to develop fully. We will show that the long-range, often highly anisotropic, interactions in the buckled phase can favor buckling of a pair of nodes in opposite directions. Buckling of these nodes can be described by randomly placed Ising-like degrees of freedom, with antiferromagnetic interaction. Thus, frustration will play an important role in the conformation of these membranes in the buckled phase, much as in spin systems with (long-range) random antiferromagnetic exchange [7,8]. Ising spin-glass behavior seems likely at low temperature, which may provide a plausible explanation of the wrinkling transition reported in Ref. [3].

The balance of our paper is as follows. We review some results of the theory of membrane buckling in Sec. II, and establish a connection with the Landau theory of second-order transitions. In Sec. III, we study isolated grain boundaries and grain-boundary networks within the continuum elastic theory of membranes. Our findings are supported by numerical simulations presented in Sec. IV, and we conclude in Sec. V with a discussion of simplified models based on this work.

II. BUCKLING OF ELASTIC MEMBRANES

We begin by reviewing the continuum theory of elastic membranes [9]. Let the shape of a membrane be parametrized by a three-dimensional displacement vector with respect to a reference plane (x, y) , and let \mathbf{u} and f be the in-plane and out-of-plane components, respectively. The energy of the membrane in a given configuration is the sum of a stretching and a bending term,

$$\begin{aligned} F &= F_s + F_b, \\ F_s &= \frac{1}{2} \int d^2r (2\mu u_{ij}^2 + \lambda u_{ii}^2), \\ F_b &= \frac{1}{2} \kappa \int d^2r (\nabla^2 f)^2. \end{aligned} \quad (2)$$

Summations over repeated indices are understood. Here κ is the bending rigidity, λ and μ Lamé coefficients, and the strain tensor is given by

$$u_{ij} = \frac{1}{2} (\partial_i u_j + \partial_j u_i + \partial_i f \partial_j f). \quad (3)$$

Note the manifest up-down symmetry ($f \rightarrow -f$). A given configuration of a fluctuating membrane occurs with probability proportional to $\exp(-F/k_B T)$.

Minimizing the energy with respect to the displacement yields the equations

$$\begin{aligned} \kappa \nabla^4 f &= \sigma_{ij} \partial_i \partial_j f, \\ \partial_i \sigma_{ij} &= 0, \end{aligned} \quad (4)$$

where the stress tensor σ_{ij} is related to the (nonlinear) strain tensor by

$$\sigma_{ij} = 2\mu u_{ij} + \lambda u_{ii} \delta_{ij}. \quad (5)$$

Because σ_{ij} is divergenceless and symmetric, it can be expressed through a single scalar potential, the Airy stress function χ :

$$\sigma_{xx} = \frac{\partial^2 \chi}{\partial y^2}, \quad \sigma_{yy} = \frac{\partial^2 \chi}{\partial x^2}, \quad \sigma_{xy} = -\frac{\partial^2 \chi}{\partial x \partial y}. \quad (6)$$

Equations of motion for the energy functional are most conveniently derived in terms of f and χ . In Cartesian coordinates, the equations, obtained originally by von Kármán, read as

$$\kappa \nabla^4 f = \frac{\partial^2 \chi}{\partial y^2} \frac{\partial^2 f}{\partial x^2} + \frac{\partial^2 \chi}{\partial x^2} \frac{\partial^2 f}{\partial y^2} - 2 \frac{\partial^2 \chi}{\partial x \partial y} \frac{\partial^2 f}{\partial x \partial y}, \quad (7a)$$

$$\frac{1}{K_0} \nabla^4 \chi = -\frac{\partial^2 f}{\partial x^2} \frac{\partial^2 f}{\partial y^2} + \left[\frac{\partial^2 f}{\partial x \partial y} \right]^2 + S(\mathbf{r}). \quad (7b)$$

Here $K_0 = 4\mu(\mu + \lambda)/(2\mu + \lambda)$ is the two-dimensional Young's modulus, and the source term, $S(\mathbf{r})$, is the total density of defects. For an isolated disclination at \mathbf{r}_0 with charge s , one has

$$S(\mathbf{r}) = s\delta(\mathbf{r} - \mathbf{r}_0), \quad (8a)$$

while for a dislocation with Burger's vector \mathbf{b} we have

$$S(\mathbf{r}) = \epsilon_{ij} b_i \partial_j \delta(\mathbf{r} - \mathbf{r}_0). \quad (8b)$$

An isolated vacancy, interstitial, or impurity atom [4] is associated with a source term

$$S(\mathbf{r}) = \frac{\Omega_0}{2\pi(1-\sigma)} \nabla^2 \delta(\mathbf{r} - \mathbf{r}_0), \quad (8c)$$

where $\sigma = \lambda/(2\mu + \lambda)$ is the 2D Poisson ratio and Ω_0 the area change associated with the defect. Other defects may be regarded as dislocation or disclination multipoles.

An effective free-energy functional for the normal displacement f can be obtained by integrating out the in-plane displacement field \mathbf{u} . The result is [10]

$$\begin{aligned} \mathcal{F} = & \frac{1}{2} K_0 \int d^2r [\nabla^{-2}(K(\mathbf{r}) - S(\mathbf{r}))]^2 \\ & + \frac{1}{2} \kappa \int d^2r (\nabla^2 f)^2, \end{aligned} \quad (9)$$

where $K(\mathbf{r}) \equiv (\partial^2 f / \partial x^2)(\partial^2 f / \partial y^2) - (\partial^2 f / \partial x \partial y)^2$ is the Gaussian curvature of the membrane at point \mathbf{r} .

This clearly displays that the free energy is the sum of two competing terms. One, proportional to Young's modulus K_0 , favors configurations where the membrane buckles out of the plane to screen out the source term. The other, proportional to the bending rigidity, favors configurations with minimum mean curvature, that is, the flat state. A buckling instability is then expected to occur, for a given source term, as the ratio K_0/κ increases, or, for given elastic constants, as the strength of the source increases. Because the stretching energy of isolated dislocations and disclinations in flat space diverges with system size, buckling occurs immediately for these defects for all values of the elastic constants in an infinite system.

The von Kármán equations are extremely difficult to solve, and most of what we know on the buckling of isolated defects was obtained by numerical simulations. One

can, however, make rigorous arguments about the buckling transition, mainly through linear stability analysis. Observe that, if the energy of a given configuration $S(\mathbf{r})$ is finite in flat space, then for small but finite K_0 the flat phase will be stable. Then $f \equiv 0$, and one can solve for the Airy stress function of the flat state χ_f ,

$$\nabla^4 \chi_f = K_0 S(\mathbf{r}). \quad (10)$$

Stability with respect to out-of-plane buckling then demands that the linear eigenvalue problem

$$\left[\kappa \nabla^4 - \frac{\partial^2 \chi_f}{\partial y^2} \frac{\partial^2}{\partial x^2} - \frac{\partial^2 \chi_f}{\partial x^2} \frac{\partial^2}{\partial y^2} + 2 \frac{\partial^2 \chi_f}{\partial x \partial y} \frac{\partial^2}{\partial x \partial y} \right] f_\eta = \eta f_\eta \quad (11)$$

admit only non-negative eigenvalues η . Equivalently, we see that, as the ratio K_0/κ increases, a buckling instability will set in as soon as an eigenvalue η becomes negative ($\eta = 0^-$). To this eigenvalue corresponds a stable configuration $f_\eta(\mathbf{r}) \neq 0$: the up-down symmetry is now broken. Thus, $f_\eta(\mathbf{r})$ can be regarded as the order parameter of a Landau theory that describes the buckling transition. The Landau free energy, given by Eq. (9), contains terms quadratic and quartic in f . Suppose for simplicity that K_0 is fixed (it can always be scaled out of the problem). Then the buckling instability is reached by decreasing κ from infinity to a critical value, κ^* .

It is easy to see that the behavior of $f(\mathbf{r})$ near the critical point is that expected from Landau theory. Let $\hat{f}_\eta(\mathbf{r})$ be the normalized eigenfunction of Eq. (11) obtained at the critical point $\kappa = \kappa^*$. Below the buckling transition, but sufficiently close to it ($\kappa = \kappa^* - \delta\kappa$, $\delta\kappa \ll \kappa^*$), we look for a solution of the von Kármán equations of the form

$$\begin{aligned} \chi(\mathbf{r}) &= \chi_f(\mathbf{r}) + \delta\chi(\mathbf{r}), \\ f(\mathbf{r}) &= \alpha \hat{f}_\eta(\mathbf{r}), \end{aligned} \quad (12)$$

where α is a scalar Ising-like order parameter. We immediately find

$$\delta\chi(\mathbf{r}) = -\alpha^2 K_0 \nabla^{-4} \hat{K}(\mathbf{r}), \quad (13)$$

where $\hat{K}(\mathbf{r})$ is the Gaussian curvature of $\hat{f}_\eta(\mathbf{r})$. Multiplying Eq. (11) on the left by $\alpha^{-1} \hat{f}_\eta(\mathbf{r})$ and integrating over all space, we find [putting $\Gamma(\mathbf{r}) \equiv K_0 \nabla^{-4} \hat{K}(\mathbf{r})$]

$$-\delta\kappa \int d^2r \hat{f}_\eta \nabla^4 \hat{f}_\eta + \alpha^2 \int d^2r \hat{f}_\eta \left[\frac{\partial^2 \Gamma}{\partial y^2} \frac{\partial^2}{\partial x^2} + \frac{\partial^2 \Gamma}{\partial x^2} \frac{\partial^2}{\partial y^2} - 2 \frac{\partial^2 \Gamma}{\partial x \partial y} \frac{\partial^2}{\partial x \partial y} \right] \hat{f}_\eta = -\eta \equiv 0, \quad (14)$$

and, thus, $\alpha \propto (\delta\kappa)^{1/2}$.

III. GRAIN-BOUNDARY BUCKLING

Grain boundaries are interfaces joining continuously two crystalline domains, A and B , of different orientation (see Fig. 2). Consider a reference lattice, e.g., the infinite extension of domain A . Domain B can be obtained by rotating A through an angle θ about the vertical. Con-

sider a closed contour in the reference lattice. If the part that lies in B is rotated as described above, and the contour encloses a segment of length h of the grain boundary, the contour will fail to close by an amount [6]

$$b = 2h \sin \frac{\theta}{2}. \quad (15)$$

Thus, dislocations must lie along the grain boundary, with Burger's vector density determined by the tilt angle

θ . Dislocations need not all have the same Burger's vector (as long as it has the proper magnitude and direction on average), but in the simplest case of a symmetric grain boundary, the boundary is equivalent to an infinite row of identical, equally spaced dislocations. We begin by studying this case in detail.

Consider a membrane with a density of defects consisting of a row of dislocations, lying on the y axis, with Burger's vectors \mathbf{b} :

$$S(\mathbf{r}) = \left[b_x \frac{\partial}{\partial y} - b_y \frac{\partial}{\partial x} \right] \delta(x) \sum_{n=-\infty}^{\infty} \delta(y - nh). \quad (16)$$

The Airy stress function in flat space is obtained from Eq. (10),

$$\begin{aligned} \chi(\mathbf{r}) = & -b_y K_0 \frac{x|x|}{4h} + b_y K_0 \frac{1}{4\pi} \sum_{n=1}^{\infty} \frac{1}{n} \exp(-2\pi n|x|/h) x \cos(2\pi ny/h) \\ & - b_x K_0 \frac{1}{4\pi} \sum_{n=1}^{\infty} \frac{1}{n^2} \exp(-2\pi n|x|/h) \left[\frac{h}{2\pi} + n|x| \right] \sin(2\pi ny/h). \end{aligned} \quad (17)$$

The requirement that the energy per unit length of the boundary be finite implies, in flat space, the well-known condition that there be no net component of the Burger's vector parallel to the boundary; i.e., $b_y = 0$. The stresses then decay exponentially in the grains as $|x| \rightarrow \infty$,

$$\begin{aligned} \sigma_{xx} & \approx \frac{K_0 b}{2h} \exp\left[-\frac{2\pi}{h}|x|\right] \left[1 + \frac{2\pi}{h}|x| \right] \sin\left[\frac{2\pi}{h}y\right], \\ \sigma_{yy} & \approx \frac{K_0 b}{2h} \exp\left[-\frac{2\pi}{h}|x|\right] \left[1 - \frac{2\pi}{h}|x| \right] \sin\left[\frac{2\pi}{h}y\right], \\ \sigma_{xy} & \approx \frac{K_0 b}{2h} \exp\left[-\frac{2\pi}{h}|x|\right] x \cos\left[\frac{2\pi}{h}y\right]. \end{aligned} \quad (18)$$

This expression for the stress tensor can be used to perform a stability analysis according to Eq. (11). The buckling problem becomes simpler, and more physically intuitive, if we work in a zero-range approximation, which should be particularly appropriate for high-angle grain boundaries, where h is of order a few lattice constants. We expect that this approximation describes the asymptotic physics more generally in the limit $x \gg h$. In this approximation, which preserves the integrated stress, the components of the stress tensor become

$$\begin{aligned} \sigma_{xx} & \approx \frac{K_0 b}{\pi} \delta(x) \sin\left[\frac{2\pi}{h}y\right], \\ \sigma_{yy} & \approx \sigma_{xy} \approx 0. \end{aligned} \quad (19)$$

Figure 3 illustrates the physical origin of the stresses above, for the case of a 21.8° symmetric grain boundary in a triangular lattice.

Using Eqs. (6) and (19), we see that the stability problem now requires finding nontrivial solutions of the equation

$$\nabla^4 f - \frac{K_0 b}{\kappa\pi} \delta(x) \sin\left[\frac{2\pi}{h}y\right] \frac{\partial^2 f}{\partial x^2} = 0. \quad (20)$$

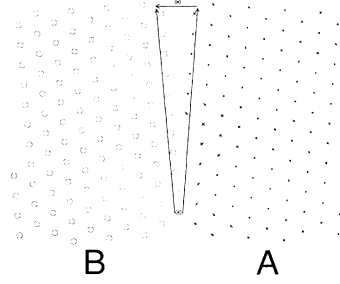


FIG. 2. Closure failure for a small-angle (9.4°) grain boundary indicating the presence of dislocations.

We look for a periodic solution in the direction of the boundary, with period h . Note that f must be of the form (up to an additive constant and a linear term in x)

$$f(\mathbf{r}) = \frac{2\pi}{h} \sum_{n=-\infty}^{\infty} f(q_n) \exp(iq_n y) \times \exp(-|q_n x|)(1 + |q_n x|), \quad (21)$$

with $q_n = 2\pi n/h$, which shows that, upon buckling, the surface remains asymptotically flat as $|x| \rightarrow \infty$. Substituting this expression for f into Eq. (20) and taking the

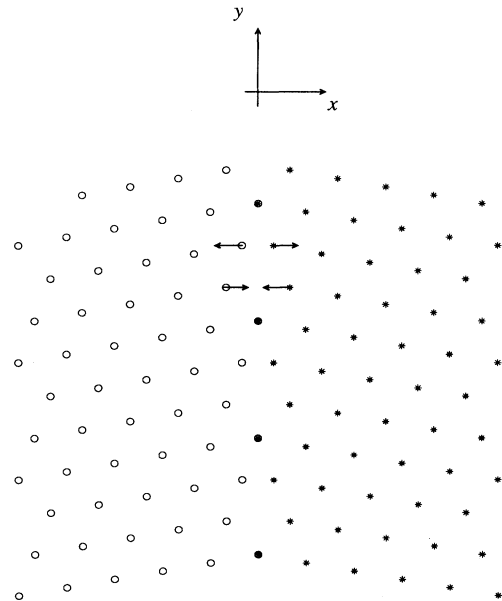


FIG. 3. Symmetric high-angle (21.8°) grain boundary in triangular lattice. The arrows display the points where the lattice is most strained. The pattern repeats itself indefinitely in the direction of the grain boundary.

Fourier transform, one obtains the following recursion relation for $q_n^2 f(q_n) \equiv \tilde{f}(q_n)$:

$$\tilde{f}(q_{n+1}) + \frac{16\pi^2}{bhK_0} |q_n| \tilde{f}(q_n) + \tilde{f}(q_{n-1}) = 0. \quad (22)$$

A buckling instability occurs when the determinant of the tridiagonal matrix defined by the recurrence first vanishes as the amplitude of the diagonal terms (i.e., of κ) is decreased from infinity. This happens for

$$\frac{16\pi^2\kappa}{bhK_0} = 0.8316, \quad (23)$$

which yields the estimate of the critical value of the elastic constants for the buckling of the zero-range model of symmetric grain boundaries

$$\frac{K_0bh}{\kappa} \approx 190. \quad (24)$$

For fixed elastic constants, this can be regarded as a condition on the tilt angle, $\theta \approx b/h$. Just below the flat space Kosterlitz-Thouless melting temperature we have $K_0b^2 = 16\pi T_{KT}$, so grain boundaries will buckle for $T \leq T_{KT}$ provided $\theta < \theta_c \approx 0.27T_{KT}/\kappa$.

The same conclusion, concerning the shape of the membrane after buckling, could be arrived at qualitatively from Eq. (2). Indeed, we note that, if buckling is to reduce the stretching energy, then the gradient of f ought to approximately cancel the components of the in-plane displacement [see Eq. (3)]. Then $|\partial_i f|$, and, thus, f itself, should decay exponentially (i.e., as the square root of the in-plane stress).

This finding appears in conflict with evidence of a long-range displacement f reported in Ref. [5], where a paper model of a grain boundary in a triangular lattice was constructed. The model is pertinent to the limit $K_0bh/\kappa \gg 1$ because of the large in-plane shear modulus. The grain boundary buckles, forms a hingelike structure with a definite dihedral angle, and displays intriguing ripples in one of the two grains. Here, we show that finite-size effects and the slight misalignment of the Burger's vectors with the grain boundary normal affect the conclusions crucially. Figure 4 displays an atomistic view of the grain boundary studied in Ref. [5]. Note that one domain is tilted by the same angle as each of the grains of Fig. 3, but the other is not. Therefore, it is no longer possible to create a stress-free configuration with coincident atomic sites: to bring the grains to match at the boundary in flat space, one has to compress uniformly (i.e., for all x) the untilted grain by a factor of $\sqrt{7}/3$ in the y direction (or to stretch the tilted grain correspondingly). If the grain is allowed out of the plane, then it can develop ripples in such a way that now the projection of the atomic rows on the plane is compressed, but the equilibrium interatomic distance in 3D space is restored. In dislocation language, this grain is characterized by Burger's vectors with a component parallel to the grain. According to Eq. (17), we have now $\sigma_{yy} \approx -b_y K_0 x / 4h |x|$, which is indeed a constant compressive load on the un-

tilted grain, and tensile load on the tilted one. When the in-plane stresses are relieved by formation of ripples in the compressed grain, stretching energy is traded for bending energy. This is certainly advantageous in a paper model, which can be easily bent and hardly stretched; if the grains are infinite, however, and if $\kappa \neq 0$, the ripples will themselves cost infinite bending energy per unit boundary length. This "infinite" energy can nevertheless still be less than the "infinite" energy of the configuration in flat space, which drives the buckling in the finite model.

Until now, we have dealt with infinite, periodic arrays of dislocations. We emphasize that periodicity played a crucial role in our arguments that grain boundary buckling does not generate any long-range out-of-plane displacement. This may not be, however, the most physically relevant situation. In fact, while grain boundaries cannot terminate inside a crystalline membrane, three or more of them can radiate outward from a common vertex. The breakdown of the periodicity of the arrays has extremely interesting consequences. We illustrate them by explicitly considering the case of three semi-infinite arrays of dislocations radiating outwards from the origin.

Let us begin by computing the shear stress produced by a half line of dislocations lying on the negative y axis, equally spaced, and with Burger's vector pointing in the x direction

$$\sigma_{xy} = K_0 b x \sum_{n=-\infty}^{-1} \frac{x^2 - (y - nh)^2}{[x^2 + (y - nh)^2]^2}. \quad (25)$$

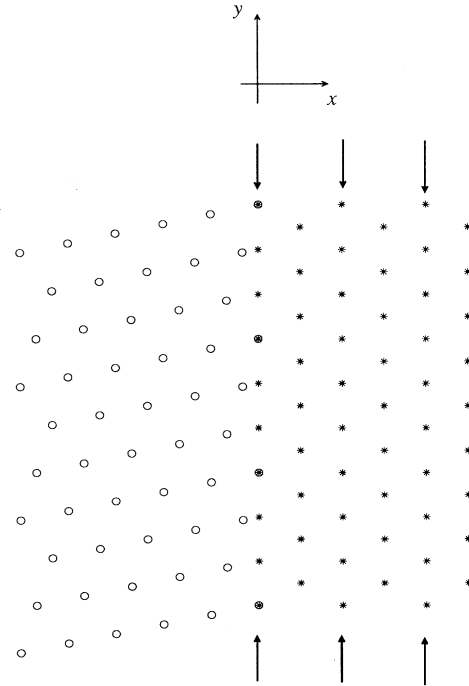


FIG. 4. Asymmetric high-angle grain boundary in triangular lattice (see also Ref. [5]). For the grains to match, a uniform compressive load must be applied to the untilted boundary.

With the aid of the Euler-Maclaurin summation formula [11],

$$\sum_{n=1}^{N-1} F(n) = -\frac{1}{2}[F(N)+F(0)] + \int_0^N dx F(x) + \int_0^N dx \left[-\sum_{n=1}^{\infty} \frac{\sin 2\pi n x}{n\pi} \right] \frac{d}{dx} F(x), \quad (26)$$

we find a multipole expansion for the shear stress field (neglecting exponentially small terms):

$$\sigma_{xy} = \frac{b}{h} x \left[-h \frac{y}{x^2+y^2} + \frac{1}{2} h^2 \frac{y^2-x^2}{(x^2+y^2)^2} - \frac{1}{6} h^3 \frac{y(y^2-3x^2)}{(x^2+y^2)^3} \right] + O(h^3/r^3). \quad (27)$$

When grain boundaries meet at a vertex, the Burger's vectors \mathbf{b}_i and dislocation spacings h_i cannot be arbitrary. This is because they determine the angles, through which the crystal orientation is rotated at each boundary (see Frank's law). Imposing the constraint that the sum of the Burger's vector densities radiating from the vertex vanish is equivalent to requiring that no net disclinity be present at the vertex, i.e., that the sum of the monopole terms of the stress field vanish. We have an additional degree of freedom at our disposal in the construction of the vertex, which is a rigid shift of the dislocations along one arm. This does not affect the monopole moment, but can be used to make the unphysical dipole terms (corresponding to a Burger's vector which is not a lattice vector) vanish. Higher-order multipoles, however, are still present. Below some critical value of the elastic constants, the vertex is stable in the flat phase, because the long-range stresses it generates are square integrable, and thus, the stretching energy is finite. Above that critical value, a buckling transition will take place to a phase with long-range out-of-plane displacements. A grain-boundary network can thus be regarded as a system of pointlike objects, the vertices where the grains intersect, with long-range, anisotropic interactions. The nature of the buckled phase of such a system is highly nontrivial, and numerical simulations suggest that spin-glass-like frustration will be important at low temperature.

IV. NUMERICAL SIMULATIONS

We have carried out numerical simulations of grain-boundary buckling, following the method described in Ref. [2]. Briefly, we work with a 2D triangular lattice of atoms, which is allowed to bend. In the ideal, unstrained crystal, each atom is sixfold coordinated, and each bond has unit length. To represent quenched defects, note that a positive (negative) disclination corresponds to a fivefold- (sevenfold-) coordinated atom, a dislocation is a disclination dipole, and so on. The stretching energy is defined as a sum over nearest-neighbor atoms,

$$F_s = \frac{\sqrt{3}}{4} K_0 \sum_{\langle i,j \rangle} (|\mathbf{R}_i - \mathbf{R}_j| - 1)^2, \quad (28)$$

where \mathbf{R} is the 3D atomic coordinate. Each elementary triangle is assigned a unit normal, \mathbf{n}_α , and the bending energy is defined as a sum over nearest-neighbor triangles,

$$F_b = \frac{2}{\sqrt{3}} \kappa \sum_{\langle \alpha, \beta \rangle} (1 - \mathbf{n}_\alpha \cdot \mathbf{n}_\beta). \quad (29)$$

The total energy is minimized, using a conjugate-gradient search [12].

First, we have studied the symmetric, high-angle grain boundary, whose unrelaxed configuration in flat space is shown in Fig. 3. Periodic boundary conditions are imposed along the grain, and free boundary conditions in the transverse direction. Figure 5(a) shows a relaxed configuration after buckling, obtained with a ratio of the elastic constants $K_0 b h / \kappa \approx 300$. We have determined numerically that the critical value of the elastic constants for this symmetric grain boundary is

$$\frac{K_0 b h}{\kappa} \simeq 120. \quad (30)$$

This value is smaller than predicted by the zero-range model, and is very close to that which would be obtained for an isolated dislocation in a membrane of finite size h .

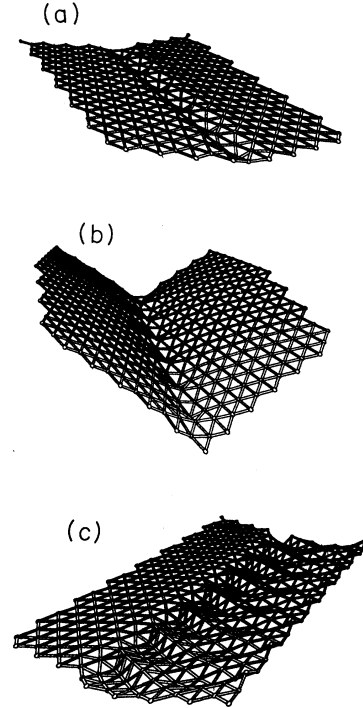


FIG. 5. (a) Buckling of a 21.8° symmetric grain boundary [the configuration in flat space is that of Fig. 3(a)]. Periodic boundary conditions have been applied in the direction of the grain boundary. (b) Same as (a), except free boundary conditions have been applied in all directions. (c) Buckling of asymmetric grain boundary (see Fig. 4 for the configuration in flat space). Periodic boundary conditions have been applied in the direction of the grain boundary.

Note that the vertical displacement never exceeds one lattice unit, and that the asymptotically flat state is reached very quickly as we move away from the grain boundary. For comparison, Fig. 5(b) shows the results of the relaxation of a *finite* segment of the same grain boundary; free boundary conditions are imposed in all directions. Now one can clearly see a long-range structure in the out-of-plane displacement, due to finite-size effects; the long-range stresses, caused by terminating the boundary freely, can be estimated from Eq. (27). Figure 5(c) shows the relaxation and buckling of the asymmetric boundary shown in Fig. 4, again with periodic boundary conditions along the boundary and free boundary conditions elsewhere. Although the ripples found in the paper model of Ref. [5] are recovered, the overall structure with periodic boundary conditions is much flatter.

These simple examples teach us that simulations of extensive grain-boundary networks would be quite challenging. Finite-size effects would make it difficult to discern the “real” effect, due to the breakdown of periodicity at a grain-boundary vertex, from the spurious effect of freely terminating each of the boundaries at the edge of the sample. Note, however, that the leading contribution to the vertex stress tensor is the quadrupole moment. A bona fide localized defect possessing the same leading multipole stress field is a tightly bound dislocation pair. This is indeed amenable to computer simulation.

The buckling of disclinations and dislocations in a tethered membrane has been investigated numerically by several authors [2,13]. Both types of defects induce large deflections in the membrane upon buckling. Figure 6 shows the buckling of a tightly bound dislocation pair. One can observe large out-of-plane displacements.

An interesting question to address concerns the shape of a membrane in the presence of more than one grain-boundary vertex, and the interaction which arises. An argument can be made that the buckling of two defects in opposite directions is favored by the bending energy (the

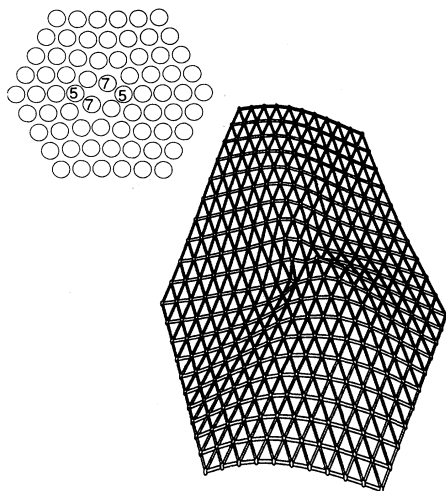


FIG. 6. Buckled tightly bound pair of dislocations with opposite Burger’s vectors (the configuration in flat space is shown in inset).

stretching energy is less important in the buckled phase) [4]. Therefore, one may expect that point defects have an “antiferromagnetic” interaction. The simplest system where this prediction can be tested is a pair of impurities consisting of atoms of a bigger size, each of which produces a spherically symmetric compression of the neighboring lattice in the flat phase, with stresses that decay as $1/r^2$. For computational purposes, these defects were embedded near the center of an approximately circular membrane (radius $R = 20$ lattice spacings, and $K_0/\kappa \approx 92$, well above the buckling transition) and the energy was minimized by constraining the defects to buckle either on the same side or on opposite sides of the flat reference configuration. Bonds radiating from the impurity atoms had equilibrium length 1.5 times the bonds in the matrix. The energy difference between the two cases is taken as an estimate of the coupling (the exchange J of an Ising model). We found that J is positive for separations below three lattice constants, and negative above that (see Fig. 7). Thus, nearest-neighbor and next-nearest-neighbor impurities have a ferromagnetic coupling, which favors buckling in the same direction, while defects farther apart have an antiferromagnetic interaction, consistent with the argument above. Note the similarity with the frustrated interactions which arise in spin glasses [8]. In real grain-boundary networks, however, we have the additional possibility of a competing *ferromagnetic* interaction between nodes connected by a buckled grain boundary.

One final feature may be important in the case of grain-boundary vertices, namely, significant anisotropy of the exchange coupling. While detailed numerical study of the coupling in this more complicated case is beyond the scope of the present work, we present the result of a simulation of pairs of interacting defects, to show that

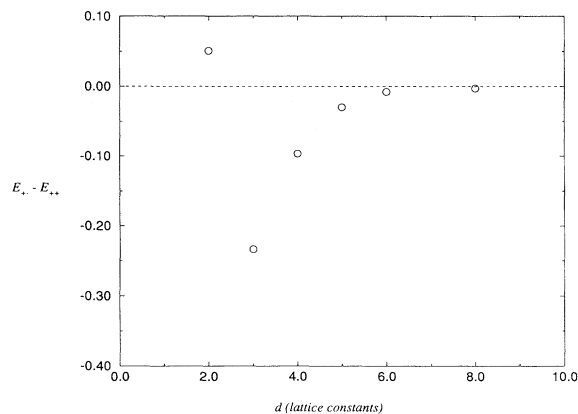


FIG. 7. Energy splitting between “antiferromagnetic” and “ferromagnetic” configurations of two impurities in an otherwise ideal crystalline membrane. Each impurity is assigned a preferred bond length which is 50% larger than the lattice constant. An isolated impurity has a buckling transition for $K_0/\kappa \geq 8$; here, we have taken $K_0/\kappa = 92$ (the lattice spacing is set to unity). When the impurities are farther apart than two lattice sites, buckling in opposite direction is energetically favored. The energy is given in units of the bending rigidity κ .

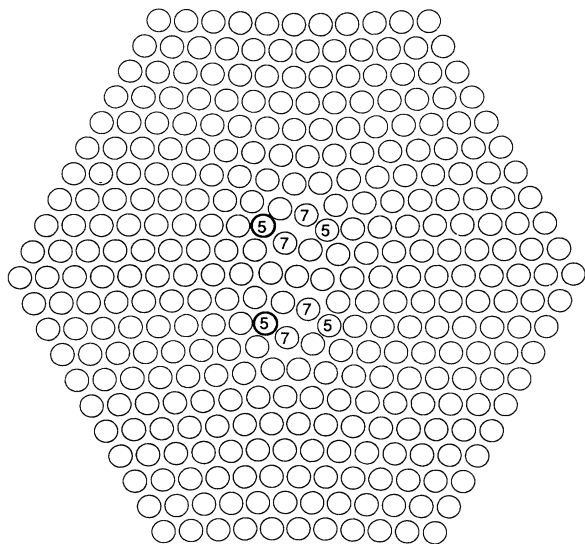


FIG. 8. Two tightly bound dislocation pairs in flat space. Explicitly marked are the fivefold- and sevenfold-coordinated atoms. The unevenly spaced atoms reside in regions of high local strain.

the basic conclusion, i.e., an antiferromagnetic interaction between defects, is still valid. Figure 8 displays the topology of a membrane containing two “nodes,” each modeled as a tightly bound dislocation pair. Each pair can be viewed as a collapsed (i.e., anisotropic) vacancy in a triangular lattice. The ratio of the elastic constants is $K_0 b^2 / \kappa \approx 92$, well above the buckling transition of an isolated pair, which we have found to occur for $K_0 b^2 / \kappa \approx 26$. The relaxation was effected subject to the

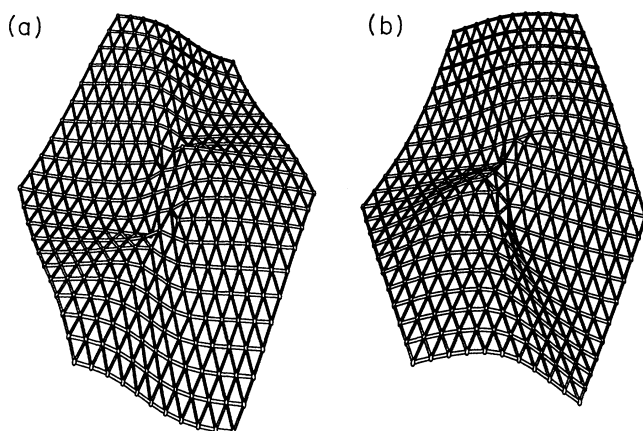


FIG. 9. (a),(b) Relaxed configuration of a membrane comprising two tightly bound dislocation pairs (see Fig. 8 for the unrelaxed configuration). The relaxation was effected subject to the constraint that the fivefold-coordinated atoms (marked by a thicker circle in Fig. 8) buckle (a) in the same or (b) in opposite direction. The total energy is 9% smaller in the latter case, indicating an “antiferromagnetic” interaction between defects.

constraint that the five-fold-coordinated atoms marked by thicker circles in Fig. 8 buckle in the same [Fig. 9(a)] or in opposite [Fig. 9(b)] direction. The fivefold atoms nearest to these heavy circles buckle oppositely to their neighbors as in Fig. 6. The total energy is 9% smaller in Fig. 9(b), indicating an antiferromagnetic interaction between these defects for this separation.

V. DISCUSSION

In conclusion, we hope to have clarified the way in which frustration arises in grain-boundary networks. Particularly important are the *nodes*, which lead to long-range strain fields and large out-of-plane displacements upon buckling. An infinite grain boundary by itself produces relatively small, exponentially screened deflections below the buckling transition. The stronger “antiferromagnetic” interaction between the buckled nodes across a grain competes with a ferromagnetic nodal interaction which presumably arises when a buckled grain boundary connects two nearest-neighbor nodes.

In studies of spin glasses, one often considers simplified theoretical models, abstracted from the complexities of real quantum-mechanical spins interacting via, say, a Ruderman-Kittel-Kasuya-Yosida interaction [8]. Similar simplifications may be appropriate for grain boundary networks in membranes. A “direct” simulation of this problem might involve quenching a flat-space liquid to produce grains, tethering neighboring particles to prevent further changes in topology, and then annealing and relaxing the resulting membrane in three dimensions. The free boundary conditions natural in this approach would lead to additional long-range strain fields (and further warping of the surface) whenever a boundary terminates at the membrane edge. Sample sizes much larger than the grain would be required to accurately model the experiment of Ref. [3], although even relatively small systems would be of some interest. One might also try to simulate grain boundary networks in membranes with a *spherical* topology, similar to the liposomes of Ref. [3].

In view of the complexity of direct simulations, it may be worth considering simplified models. One approach would be to deliberately insert vacancies and interstitials into an otherwise perfect membrane (to simulate nodes), and ignore the exponentially screened grain boundaries entirely. Such a model would be similar to the random-impurity model discussed in Ref. [4]. For weak disorder, the equilibrium flat phase [2] survives at finite temperatures (with microscopic buckling at small scales), although there are indications of a spin-glass phase when the disorder is strong [14]. Glassy behavior at low temperatures has been found in computer simulations [15]. One could abstract even further and simply replace the buckled defects by Ising degrees of freedom with effective Hamiltonian

$$\mathcal{H}_{\text{eff}} = - \sum_{\substack{i,j \\ i < j}} J(|\mathbf{r}_i - \mathbf{r}_j|) \sigma_i \sigma_j, \quad (31)$$

where $\sigma_i = \pm 1$, the $\{\mathbf{r}_i\}$ are random positions within the membrane, and $J(r)$ has the form shown in Fig. 7. Simple power counting using Eq. (2) suggests that the antiferromagnetic tail of $J(r)$ has the form $J(r) \approx -\kappa/r^2$. Even the behavior of this simple two-dimensional Ising spin glass is, to the best of our knowledge, unknown.

ACKNOWLEDGMENTS

We acknowledge helpful discussions with G. Grest and D. Huse. This work was supported by the National Science Foundation, through Grant No. DMR91-15491, and through the Harvard Materials Research Laboratory.

-
- [1] D. R. Nelson and B. I. Halperin, *Phys. Rev. B* **19**, 2457 (1979).
 - [2] H. S. Seung and D. R. Nelson, *Phys. Rev. A* **38**, 1005 (1988).
 - [3] M. Mutz, D. Bensimon, and M. J. Brienne, *Phys. Rev. Lett.* **67**, 923 (1991).
 - [4] D. R. Nelson and L. Radzihovsky, *Europhys. Lett.* **16**, 79 (1991); L. Radzihovsky and D. R. Nelson, *Phys. Rev. A* **44**, 3525 (1991); D. Bensimon, D. Mukamel, and L. Peliti, *Europhys. Lett.* **18**, 269 (1992).
 - [5] D. R. Nelson and L. Radzihovsky, *Phys. Rev. A* **46**, 7474 (1992); this paper also argues that unscreened *disclinations*, quenched in by the polymerization process, would lead to a wrinkled glass. We exclude this possibility here, and concentrate on grain-boundary networks with no unscreened disclenicity.
 - [6] J. P. Hirth and J. Lothe, *Theory of Dislocations* (Wiley, New York, 1992).
 - [7] A. P. Young, J. D. Reger, and K. Binder, *Theor. Appl. Phys.* **71**, 355 (1992).
 - [8] K. H. Fischer and J. A. Hertz, *Spin Glasses* (Cambridge University Press, Cambridge, 1991).
 - [9] A more extensive discussion can be found in Ref. [2]. The basic equations of the theory of elastic membranes are the same as in the theory of thin plates; see, e.g., L. D. Landau and E. M. Lifshitz, *Theory of Elasticity* (Pergamon, New York, 1970).
 - [10] D. R. Nelson and L. Peliti, *J. Phys. (Paris)* **48**, 1085 (1987).
 - [11] K. Knopp, *Theorie und Anwendung der Unendlichen Reihen* (Springer, Berlin, 1964), p. 540.
 - [12] W. H. Press, B. P. Flannery, S. A. Teukolsky, and W. T. Vetterling, *Numerical Recipes* (Cambridge University Press, Cambridge, 1986), Chap. 10.
 - [13] D. C. Morse and T. C. Lubensky, *J. Phys. (France) II* **3**, 531 (1993).
 - [14] L. Radzihovsky and P. Le Doussal, *J. Phys. (France) I* **2**, 599 (1992).
 - [15] Y. Kantor, *Europhys. Lett.* **20**, 337 (1992).